eLIFE elifesciences.org

RESEARCH ARTICLE

Figures and figure supplements

The genome and phenome of the green alga *Chloroidium sp.* UTEX 3007 reveal adaptive traits for desert acclimatization

David R Nelson *et al*

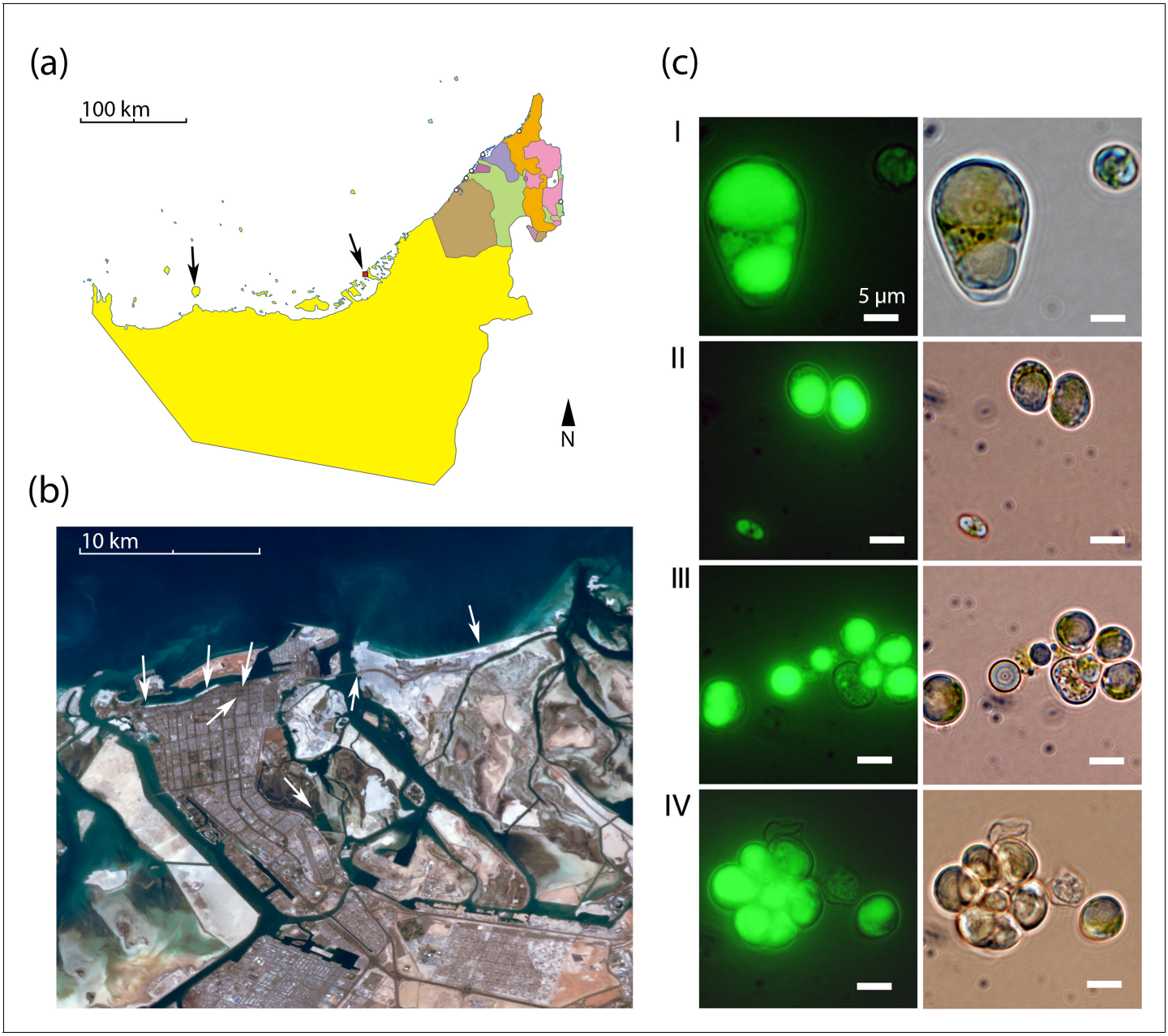

Figure 1. Geography and morphology of isolated *Chloroidium* strains. *Chloroidium* strains were isolated from samples taken from the indicated locations in (**a**) the UAE, and (**b**) within Abu Dhabi city specifically. *Chloroidium* strains were found in estuaries, mangrove forests, adhered to buildings, in municipal waters, etc. (**c**) *Chloroidium sp. UTEX 3007* stained for lipid bodies with BODIPY 505/515 and observed by fluorescence microscopy (left column) and phase-contrast microscopy (right column). (**I**) *Chloroidium sp. UTEX 3007* aplanospore displaying palmello-like morphology contrasted with a smaller vegetative cell, (II) two average-sized *Chloroidium sp. UTEX 3007* cells can be seen in the upper right of the panel while a miniature, recently hatched from an autospore, can be seen in the lower left, (III) Stained oil stores excreted from a *Chloroidium sp. UTEX 3007* cell, and (IV) a hatched, non-segregating autospore.

DOI: 10.7554/eLife.25783.003

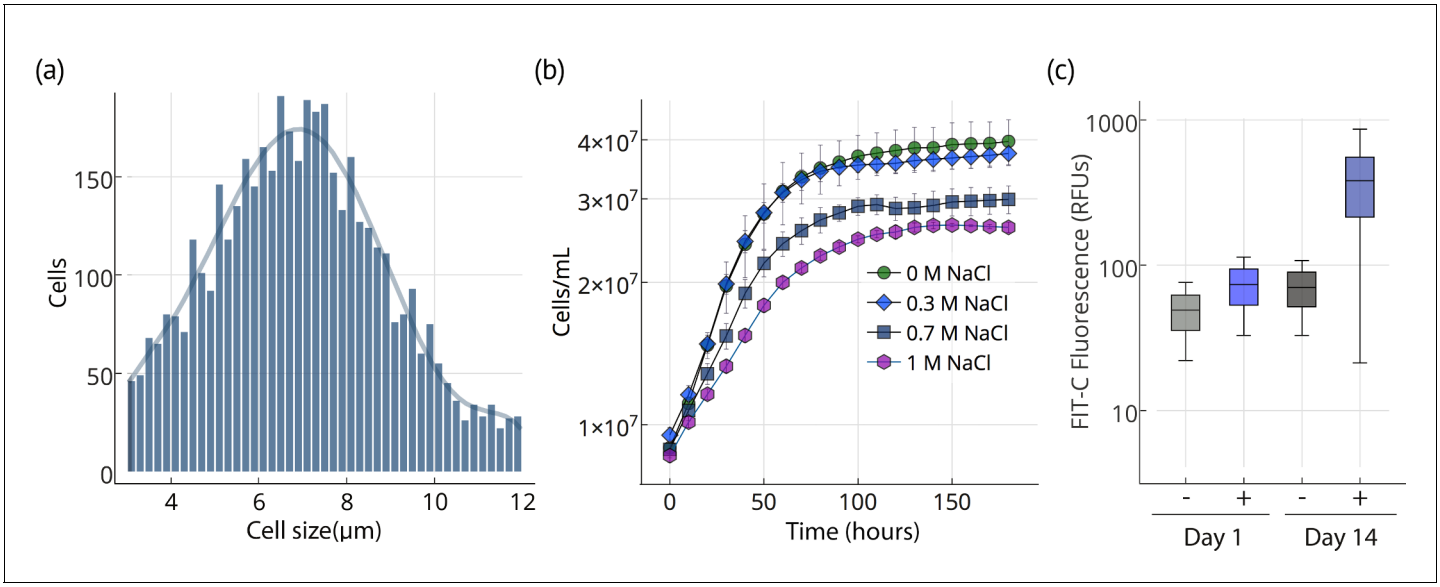

Figure 2. Cell size, growth, and lipid accumulation in *Chloroidium sp. UTEX 3007*. (**a**) Cell size distribution of *Chloroidium sp. UTEX 3007* in late log phase (14 days). Cell size analysis was performed using a Cellometer Auto M10 from Nexcelcom Bioscience (Lawrence, MA, USA) on 2 × 20 ul from each liquid algal sample. As autospores typically generate six progeny, the distribution was fitted with the sixth order polynomial equation: (a + b*x + $c*x^2$ + $d*x^3$ + $e*x^4$ + $f*x^5$ + $g*x^6$). (**b**) Growth of *Chloroidium sp. UTEX 3007* cultures in tris-minimal media supplemented with 0, 0.3, 0.7. and 1M NaCl at 20˚C and 400 umol photons m^{-m} s^{-s} of full-spectrum light). Cells were grown in a Multi-Cultivator MC 1000 by Photon Systems Instruments (Drasov, Czech Republic. See ***Figure 2—figure supplement 2*** for chlorophyll/cell count curve and ***Figure 2—figure supplement 1*** for a growth curve in the open pond simulators (OPSs). (**c**) Fluorescence intensity of cells (RFUs=relative fluorescence units) measured with a BD FACSAria III flow cytometer (BD Biosciences, San Jose, CA) at mid-log phase (time=day 1, one week after inoculation) and one week into stationary phase (time=day 14) with and without staining (indicated as (+) or (-), respectively, from the lipophilic dye BODIPY 505/515. Whiskers indicate range, box edges indicate standard deviation and the box centerline indicates the median fluorescence intensity reading.

DOI: 10.7554/eLife.25783.004

The following source data is available for figure 2:

Source data 1. Cell diameter measurements.

DOI: 10.7554/eLife.25783.005

Source data 2. Cell concentration time course measurements.

DOI: 10.7554/eLife.25783.006

Source data 3. Flow cytometry measurements.

DOI: 10.7554/eLife.25783.007

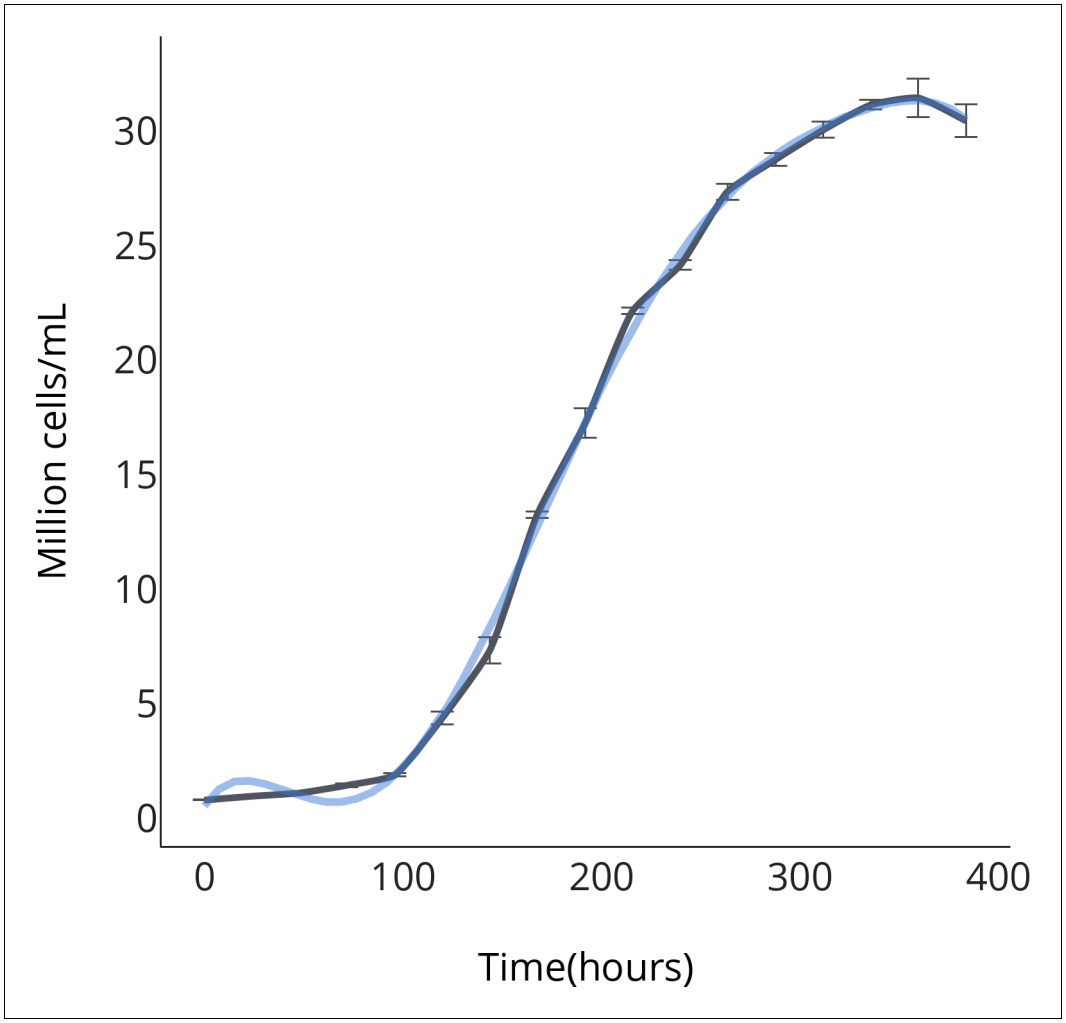

Figure 2—figure supplement 1. OPS growth curve.
DOI: 10.7554/eLife.25783.008

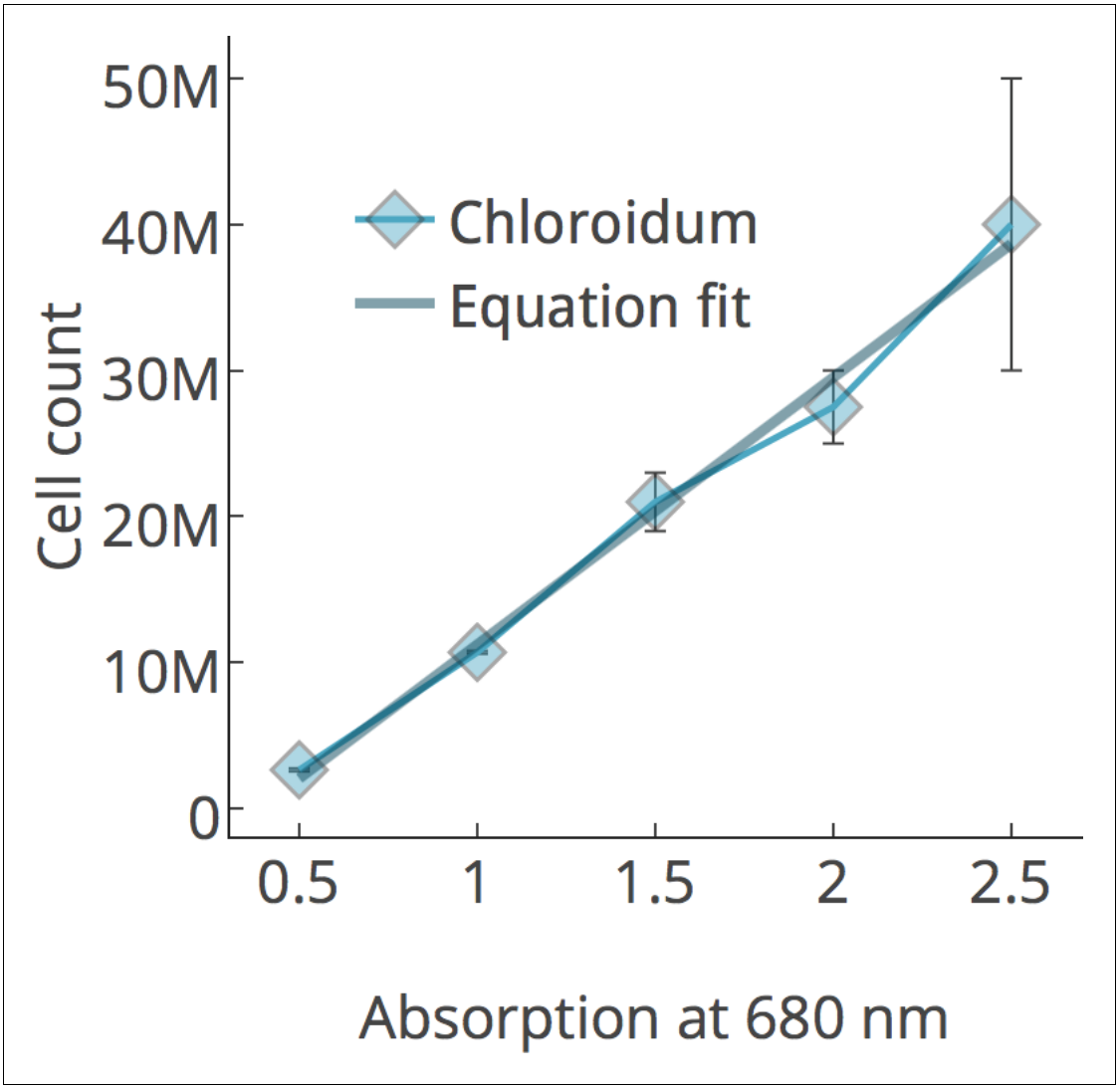

Figure 2—figure supplement 2. Chlorophyll/cell count curve.
DOI: 10.7554/eLife.25783.009

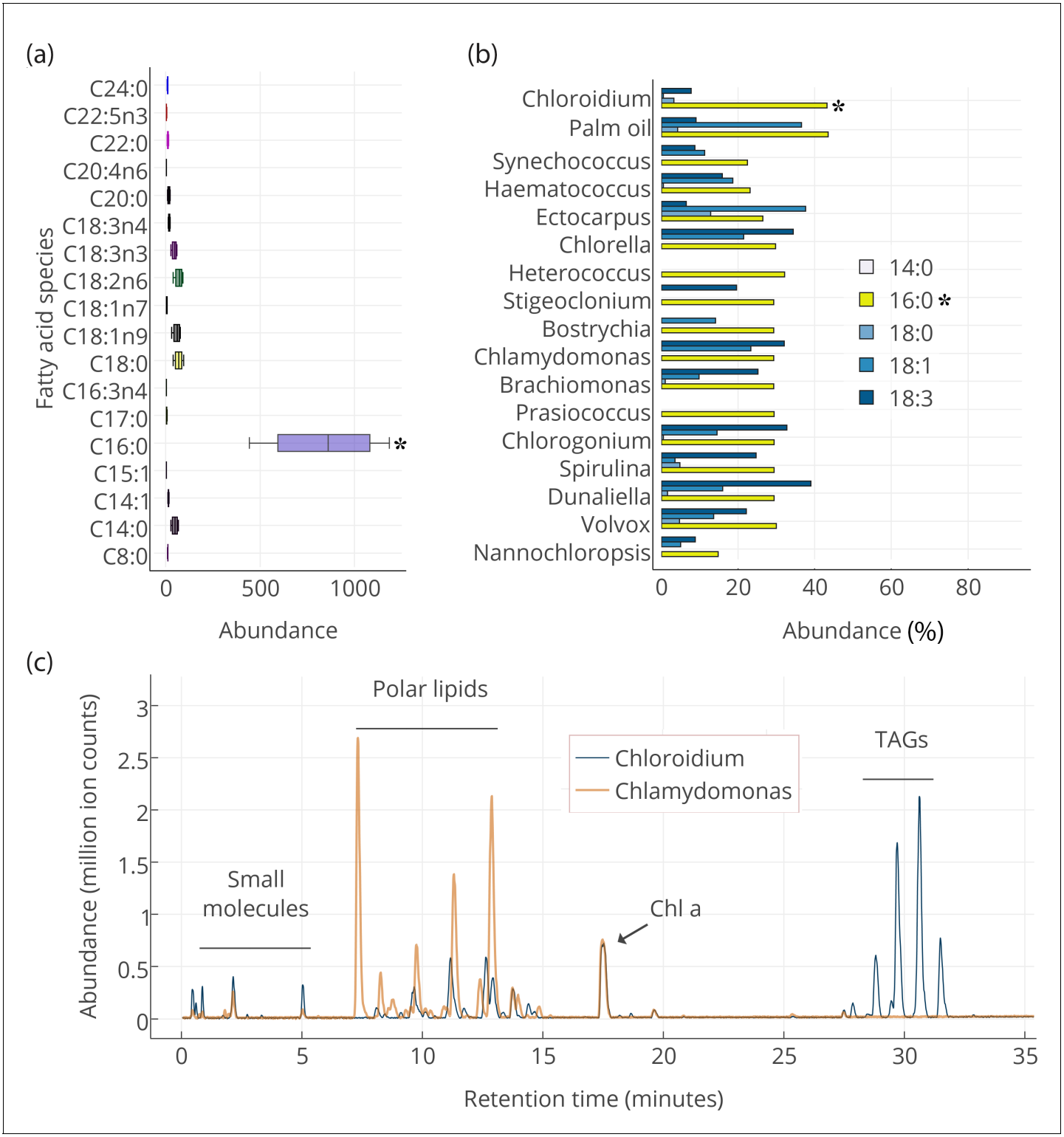

Figure 3. Lipid composition of *Chloroidium sp. UTEX 3007* observed with HPLC/MS and GC-FID, and comparison with other photosynthetic, oleagenic species. (**a**) *Chloroidium sp. UTEX 3007* fatty acid content estimated by extracting total lipid, creating methyl esters, and running the esters on a GC-FID (whiskers = range, box boundaries = 1 SD, center box line = mean [8 replicates]). (**b**) Comparison of fatty acid profile of *Chloroidium sp. UTEX 3007* with that of oil palm (*Elaeis guineensis*) (***Barcelos et al., 2015***) and several other algal isolates (***Lang et al., 2011***). Asterisks mark the presence of palmitic acid in *Chloroidium sp. UTEX 3007*. (**c**) Base peak chromatograms (BPCs) from stationary phase *Chloroidium sp. UTEX 3007* and *Chlamydomonas reinhardtii* extracts run in positive mode on an Agilent LC-MS QToF 6538 (Agilent, Santa Clara, CA, USA) using an acetonitrile/

Figure 3 continued on next page

Figure 3 continued

ammonium formate/isopropanol gradient. Cultures were grown for three weeks in F/2 media with 0 g/L NaCl (freshwater media). Triacylglycerols (TAGs) can be seen in abundance in *Chloroidium sp. UTEX 3007* while *Chlamydomonas reinhardtii* contained a higher ratio of polar lipids (Dataset 2).
DOI: 10.7554/eLife.25783.010
The following source data is available for figure 3:

Source data 1. GC-FID results for major fatty acid species in *Chloroidium sp.* UTEX 3007.
DOI: 10.7554/eLife.25783.011
Source data 2. Fatty acid profiles of *Chloroidium sp. UTEX 3007*, *Elaeis guineensis* (***Barcelos et al., 2015***), and several other algal isolates (***Lang et al., 2011***).
DOI: 10.7554/eLife.25783.012
Source data 3. HPLC-MS base peak chromatograms (BPCs) for *Chloroidium sp. UTEX 3007* and *Chlamydomonas reinhardtii* extracts.
DOI: 10.7554/eLife.25783.013

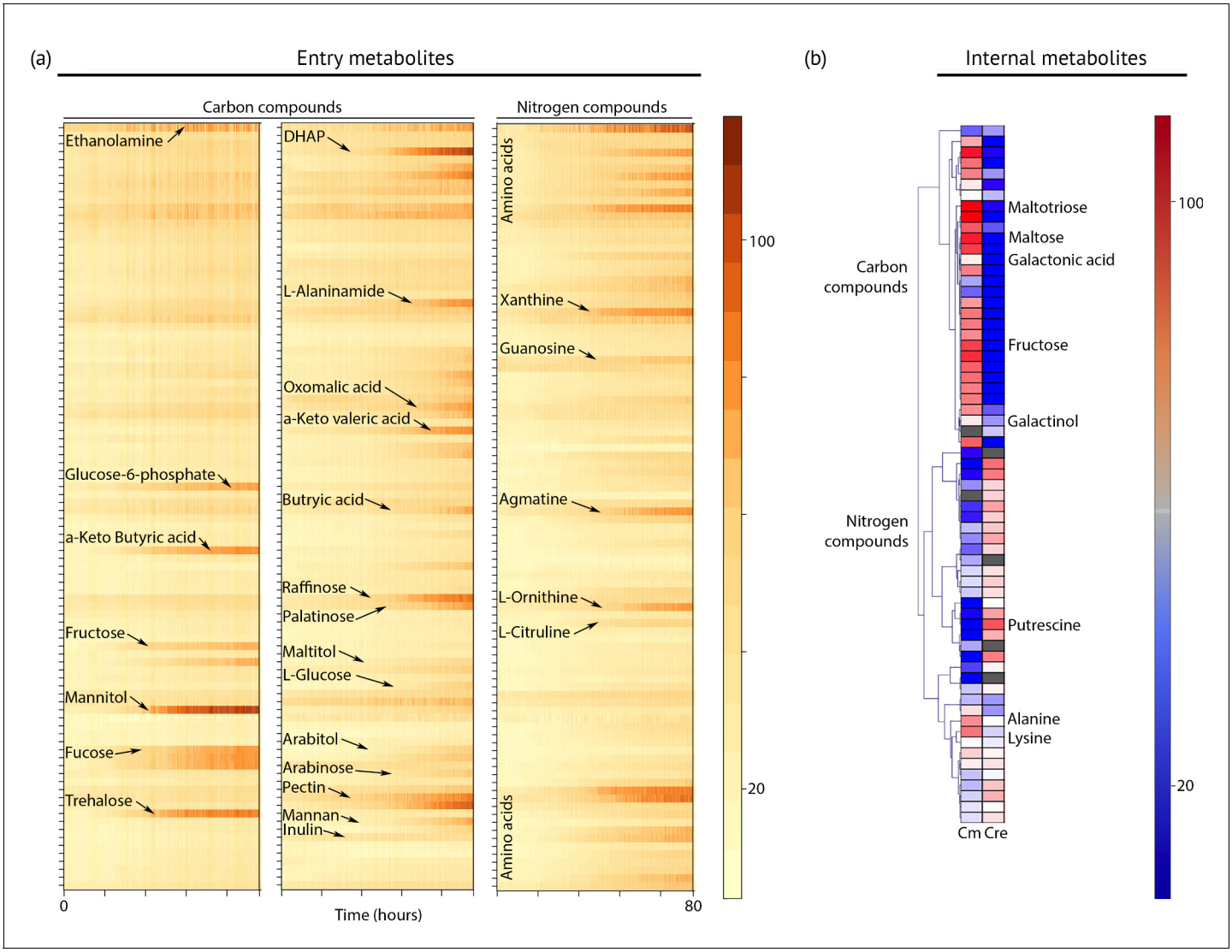

Figure 4. Metabolic profiling of *Chloroidium sp. UTEX 3007*. (**a**) Biolog phenotype microarrays were run using an Omnilog instrument (Biolog Inc., Hayward, USA) as previously described (***Chaiboonchoe et al., 2014***). In total, 380 substrate utilization assays for carbon sources (PM01 and PM02 plates), 95 substrate utilization assays for nitrogen sources (PM03 plate), 59 nutrient utilization assays for phosphorus sources, and 35 nutrient utilization assays for sulfur sources (PM04 plate), along with peptide nitrogen sources (PM06-08 plates) were performed (Dataset 2). All microplates were incubated at 25°C for up to 8 days, and the dye color change (in the form of absorbance) was read with the Omnilog system every 15 min. As the Omnilog instrument does not provide a source of continuous light during incubation, the algae are assumed to be carrying out heterotrophic respiration. In addition, a marked increase in the chlorophyll *a* content and total cell count was confirmed for wells with suggested growth. Kinetic curves were plotted from the raw data in the form of heatmaps, and statistical analysis was carried out to visualize the metabolic properties and generate Omnilog values. Heatmap density correlates to Omnilog-registered color density. In addition to the dye color change, Omnilog also registers color change resulting from the accumulation of other pigments, including chlorophyll *a*. Thus, growth is displayed as cumulative color change density. (**b**) Extraction and analysis by gas chromatography coupled with mass spectrometry was performed as described in ***Lisec et al. (2006)***. The color scale corresponds to chromatogram peak areas reported in the GC-MS results in **Dataset 2**. Significant increase of diverse carbon compounds was observed in *Chloroidium sp. UTEX 3007* (Cm) as compared to *Chlamydomonas reinhardtii* (Cre), and vice versa for nitrogen compounds. These differences may reflect acclimatization to their respective habitats and lifestyles.

DOI: 10.7554/eLife.25783.014

The following source data is available for figure 4:

Source data 1. Phenotype microarray results for plates PM1, PM2, and PM3.

DOI: 10.7554/eLife.25783.015

Source data 2. GC-MS results for *Chloroidium sp. UTEX 3007* (Cm) and *Chlamydomonas reinhardtii* (Cre) intracellular polar metabolites.

DOI: 10.7554/eLife.25783.016

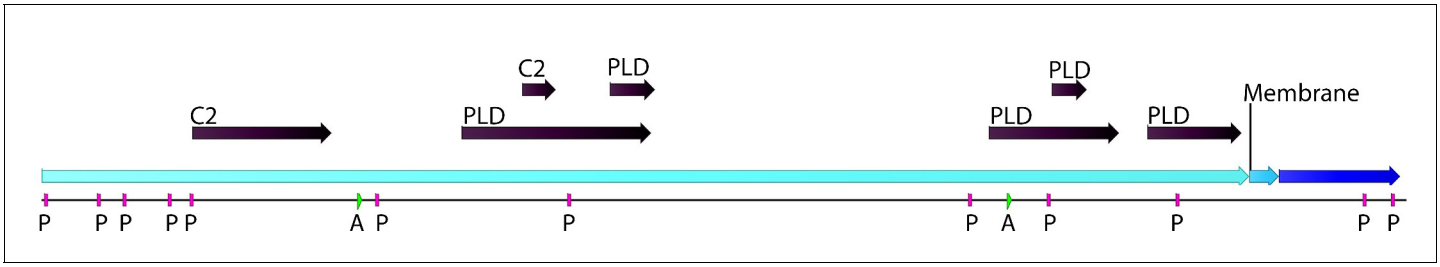

Figure 5. Phospholipase D (PLD; EC number: 3.1.1.4) domain-containing gene in *Chloroidium sp. UTEX 3007*. Functional protein family domains in a *Chloroidium sp. UTEX 3007* predicted protein with high similarity to PLD proteins from closely related organisms. PLDs are members of the phospholipase superfamily and produce phosphatidic acid as a main product. Phosphatidic acid is involved in signaling, membrane curvature, and is rapidly converted to diacylglycerol. The *Chloroidium sp. UTEX 3007* PLD contains several domains with calcium-binding, amidation, and phosphorylation sites (annotated as C2 (2), A (2), or P(11) domains). C2 domains act to target proteins to cell membranes and allow phosphatases to de-phosphorylate membrane lipids without removing them from the membrane.

DOI: 10.7554/eLife.25783.017

The following source data is available for figure 5:

Source data 1. Locations, confidence scores, and accession numbers for PLD and C2 Pfam domains in *Chloroidium sp. UTEX 3007*.

DOI: 10.7554/eLife.25783.018

(a)

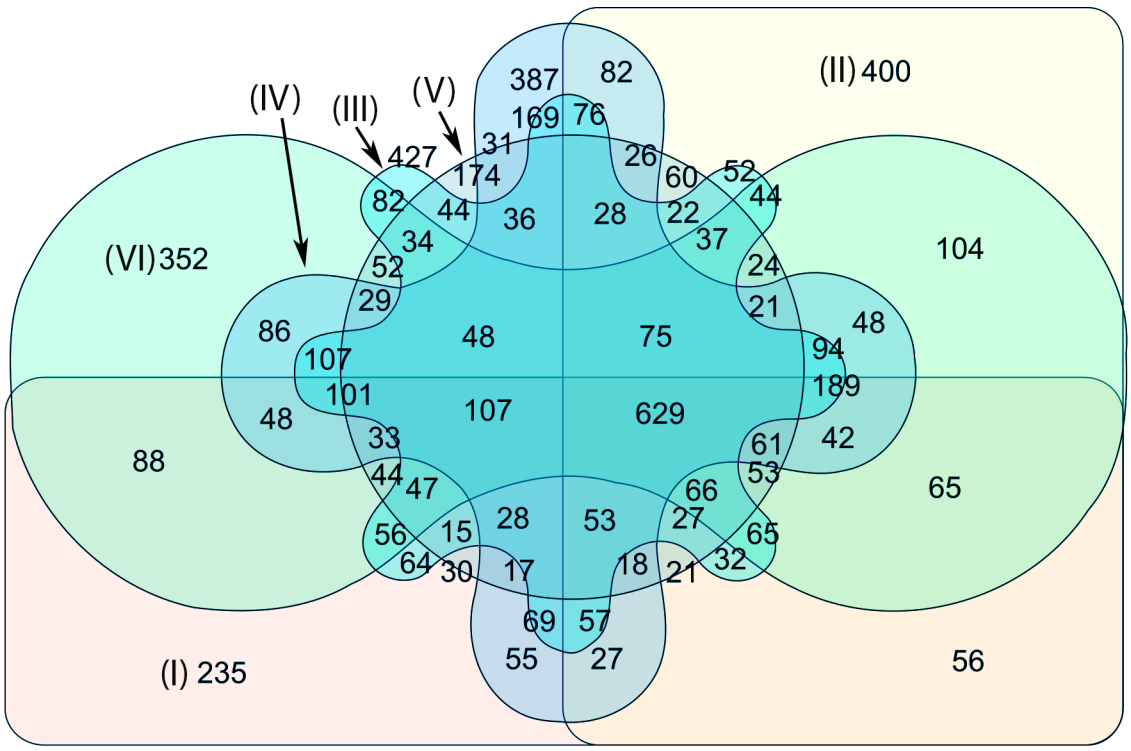

(b)

Pfam set	Assembly	Length (bp)	GC (%)	Contigs	N's/100 kbp	Pfam domains
(I)	Chloroidium sp. UTEX3077	52511570	52.38	710	92.5	9455
(II)	Chlamydomonas reinhardtii	120185366	63.93	1556	12476.55	11895
(III)	Ostreococcus taurii	12916858	59.38	20	73.86	16784
(IV)	Micromonas pusilla	21907557	65.84	58	1443.36	16466
(V)	Chlorella variabilis NC64A	46159515	67.14	414	8546.69	8156
(VI)	Coccomyxa subellipsoidea	48952548	52.93	45	0	13057

Figure 6. Protein family (Pfam) domains in *Chloroidium sp. UTEX 3007* compared with algae from other clades. Well-curated assemblies from genomes of algae from four other clades were downloaded from NCBI [assemblies - *Micromonas pusilla*, *Ostreococcus taurii*, and *Coccomyxa subellipsoidea*]. The *Chlamydomonas reinhardtii* genome was downloaded from Phytozome (v5.5) (***Merchant et al., 2007***). De novo gene prediction, including exon-intron structural modeling, yielded a set of peptide predictions that served as a base for HMM alignment with Pfam-A (v31.0, (http://hmmer.org).). (**a**) Shared and unique Pfam sets from representative species of major green algae clades. Pfam lists can be viewed by selecting the numbers displayed for each shared or unique value in ***Figure 6—source data 3***. (**b**) Legend for (**a**) including additional metrics describing the algal assemblies used for de-novo coding sequence and Pfam predictions.

DOI: 10.7554/eLife.25783.019

The following source data is available for figure 6:

Source data 1. Predicted Pfam designations for each species in ***Figure 6***.

DOI: 10.7554/eLife.25783.020

Source data 2. Table with QUAST results used in (b).

DOI: 10.7554/eLife.25783.021

Source data 3. Interactive Venn diagram that can be viewed at interactivenn.net to obtain Pfam sets for numbers displayed in ***Figure 6***.

DOI: 10.7554/eLife.25783.022

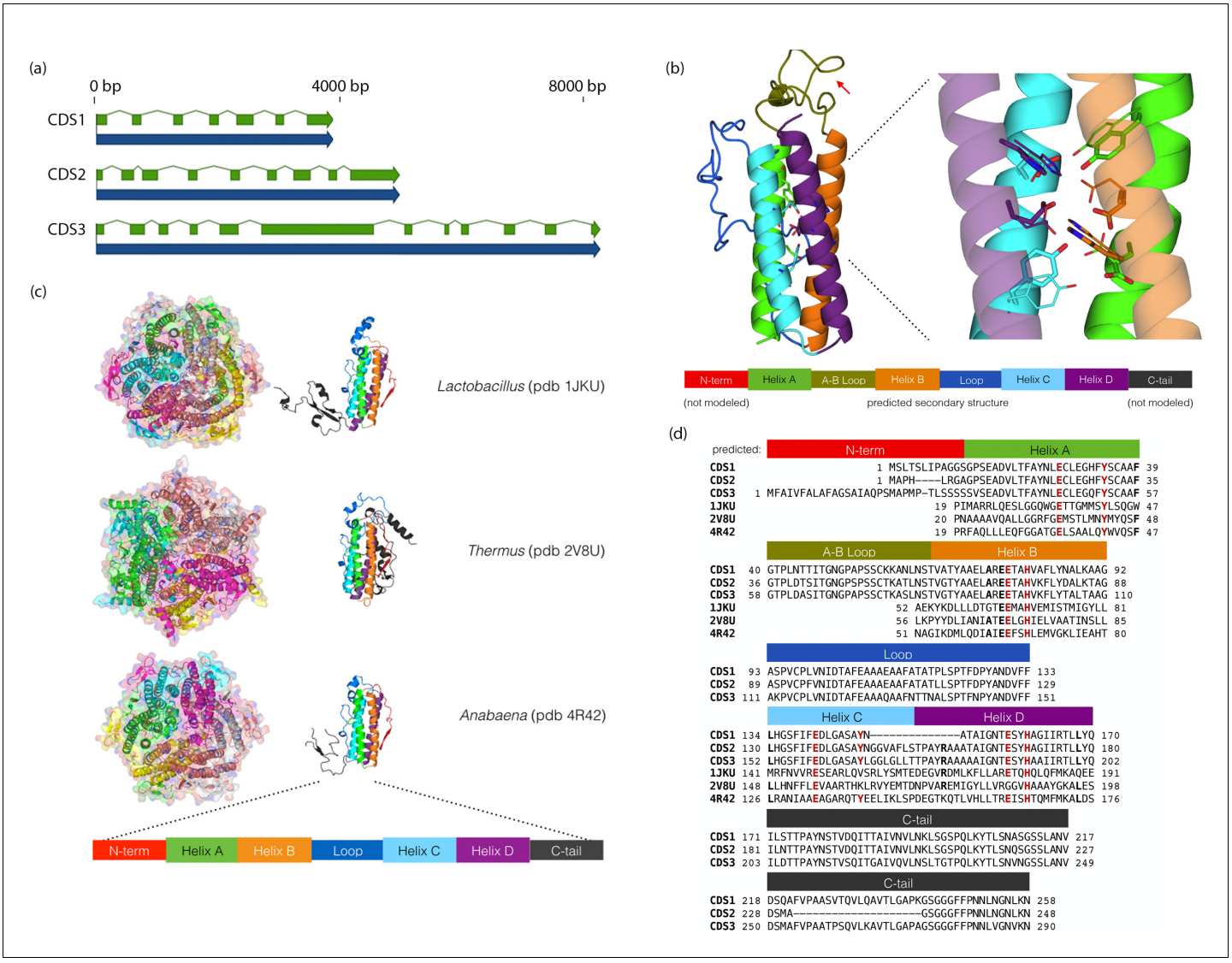

Figure 7. *Chloroidium sp. UTEX 3007* genes exhibiting homology with desiccation-responsive *Deinococcus* genes. (**a**) Gene models for the putative manganese catalases (CDS1/2/3). Functional annotation of homologs from (CDS1/2/3) is limited: 96 of the top 100 BLAST hits of CDS3 in the non-redundant database (nr v. 2.31, NCBI) are annotated as hypothetical or predicted proteins. Of the other four, three are characterized as desiccation related (from *Auxenochlorella protothecoides, Deinococcus gobiensis I-0,* and *Salinisphaera shabanensis E1L3A*). (**b**) Experimental structures of representative Mn catalases (***Antonyuk et al., 2000***; ***Barynin et al., 2001***; ***Bihani et al., 2013***) showing the homohexamers (left) and isolated monomers (right). The latter are colored according to structural motifs as given. (**c**) Left: Homology model of CDS3, colored according to linear structure shown below (the additional presumptive loop is indicated by the red arrow and the predicted Mn coordinating side chains are shown as sticks). Right: Zoom in of same homology model aligned with the metal coordinating residues of *Anabaena PCC 7120* Mn catalase (pdb 4R42); highlighting the spatial alignment of side chains (homology model side chains shown as thick sticks, 4R42 as thin sticks). (**d**) Sequence alignment of CDS1-3 shown with the predicted secondary structure. The presumptive helical regions are also aligned with the corresponding sequences from the known Mn catalase structures. Canonical Mn coordinating residues are in red and other positions with sequence identity between CDS1-3 and at two least of the known catalases are in bold.

DOI: 10.7554/eLife.25783.024

The following source data is available for figure 7:

Source data 1. Models of CDS1-3 in protein data bank (PDB) format.

DOI: 10.7554/eLife.25783.025

Source data 2. Amino acid residue alignment of CDS1-3.

DOI: 10.7554/eLife.25783.026

Dessication-associated protein [Deinococcus gobiensis I-0]

Sequence ID: gb|AFD25669.1| **Length:** 311 **Number of Matches:** 1

Score	Expect	Method	Identities	Positives	Gaps
155 bits(392)	4e-41	Compositional matrix adjust.	108/263(41%)	138/263(52%)	16/263(6%)

```
Query  34   EADVLTFAYNLECLEGQFYSCAAFGTPLDASITGNG-----PAPSSCTKASL--NSTVGT  86
            + DVL FA NLE LE  FY  AA G   +    G G     PA    T+     NS V
Sbjct  58   DGDVLNFALNLEYLEAAFY-LAAVGRVDELRAIGGGAEIRLPANLDRTRGMQFKNSNVEA  116

Query  87   YAAELAREETAHVKFLYTALTAAGAKPVCPLVNIDTAFEAAAQAAFNTTNALSPTFNPYA  146
             A ++A +E AHVKFLY AL  A A    P++++  AF+AA +AA   +      FNPYA
Sbjct  117  LARDIAEDELAHVKFLYGALGKAAAPR--PVLDLSGAFDAAGRAA---SGGKIVGFNPYA  171

Query  147  NDVFFLHGSFIFEDLGASAYLGGLGLLTTPAYRAAAAAIGNTESYHAAIIRTLLYQILDT  206
            ND+FFLHG+FIFED+G +AY G   L+T PAY  AAA I   E+YH  ++R +LY+
Sbjct  172  NDLFFLHGAFIFEDVGVTAYNGAATLITNPAYLQAAAGILAVEAYHGGVVRGMLYEQRQV  231

Query  207  TPAYNSTVSQITGAIVQVLNSLTGTPQLKYTLSNVNGSSLANVDSMAFVPAATPSQVLKA  266
            T A    V Q+  AI  +            LS+  G+  A  D  A     T  +VL
Sbjct  232  TAAAGLYVGQVIDAISAL--RGKVGGGKDVGLSDSRGAVFAPADRNAVAYPRTTREVLNI  289

Query  267  VTLGAPAGSGGGFFPNNLVGNVK  289
            V L AP  S GGF+PN L G +K
Sbjct  290  VYL-APGASKGGFYPNGLNGTIK  311
```

Figure 7—figure supplement 1. Alignment of CDS3 to a *Deinococcus globiensis* desiccation-related protein (***Yuan et al., 2012***). Metal-binding motif residues are highlighted.

DOI: 10.7554/eLife.25783.027